# Starch-Filled Ternary Polymer Composites. II: Room Temperature Tensile Properties

S. ST. LAWRENCE[1], P. S. WALIA[3], F. FELKER[2], *and* J. L. WILLETT[1]

[1]*Plant Polymer Research Unit*
[2]*Cereal Products and Food Science Research Unit*
*National Center for Agricultural Utilization Research*
*USDA-ARS**
*Peoria, IL 61604*

[3]*Engineering Sciences Polymer Processing*
*The Dow Chemical Company*
*Midland, MI 48677*

The room temperature tensile properties of granular starch-filled low-density polyethylene (PE) and starch-filled blends of PE and poly(hydroxy ester ether) (PHEE) are presented. At low filler contents ($\phi_f$), the filled PE:PHEE blend has a higher yield stress and tensile strength than either the starch/PE composites or the unfilled matrix. The increase in the yield stress indicates that matrix yielding occurs before debonding. At high filler contents, the tensile strength of the filled blend is again greater than the strength of the starch/PE composites. This increase in strength is the result of higher debonding stresses in the ternary composite. In both materials there is a change in the deformation process at a critical filler content, $\phi_{cr}$. Below $\phi_{cr}$, deformation involves the growth of debonded regions; above $\phi_{cr}$, deformation is confined to narrow damaged zones. There is a reduction in the strain at failure when this change in the deformation process occurs. Although the PHEE surface coating affects the debonding stress and the tensile strength, it does not affect the strain at failure or the tensile modulus. For both composite materials, the increase in modulus with $\phi_f$ can be adequately described using a simplified form of the Kerner equation. Polym. Eng. Sci. 44:1839–1847, 2004. 

## INTRODUCTION

Rigid fillers, such as granular starch, are added to polymers to improve certain physical properties, such as dimensional stability and stiffness (1). They often also have the added benefit of reducing cost. However, some undesirable consequences are associated with the addition of fillers, including the need for more complex fabrication techniques or a reduction in some mechanical properties such as toughness or impact strength. In an effort to minimize the undesirable effects while still taking advantage of the benefits, more complex multi-component composites have been considered (2, 3). For example, in polymers with rigid fillers, a low-modulus rubber is sometimes added to improve the toughness (4). The physical properties of such a 3-phase composite depend on the interactions between the individual components, which in turn affect the morphology (2). Two limiting cases may be considered: 1) both the filler and the minor component are dispersed separately in the continuous matrix, or 2) the minor component encapsulates the filler particles. Encapsulation occurs if it is kinetically possible and if it reduces the total interfacial energy in the composite (5–7). The presence of a surface coating on the filler particles has been shown to improve the mechanical performance of some composite materials (8). In these composites, the interaction between the matrix and the interlayer is extremely important since the ability of this material to strengthen the filler/matrix interface affects the strength, ductility and toughness of the composite (2, 8).

Biobased composites of poly(hydroxyester ether) (PHEE) with natural polymers such as starch or proteins have been an active area of research in recent

*Names are necessary to report factually on available data; however, the USDA neither guarantees nor warrants the standard of the product, and the use of the name by USDA implies no approval of the product to the exclusion of others that may also be suitable.


Published online in Wiley InterScience (www.interscience.wiley.com).
DOI: 10.1002/pen.20185

years (9–17). As part of this effort, we recently reported the dynamic mechanical properties of ternary starch/PE/PHEE composites (17). Examination of the fracture surface of broken tensile bars clearly showed the presence of a surface coating of PHEE on the starch granules in these ternary composites. This surface coating resulted in an amplification of the relaxation at the glass transition of PHEE. In this paper, it is shown that the PHEE interlayer strengthens the interface between the matrix and the filler and as a result increases the composite's tensile strength. The presence of the PHEE does not, however, adversely affect either the ductility or the stiffness.

Low-density PE was chosen for this investigation because it is immiscible with PHEE and because in a starch/PE/PHEE composite there is a strong driving force for encapsulation (based on estimates of the surface energy). The inclusion of compatibilizers or coupling agents such as octenyl succinate (18), oxidized polyethylene (19), ethylene copolymers (20–22), ionomers (23), and maleated polyethylene (24) to improve tensile properties of starch/PE composites have also been reported.

## EXPERIMENTAL

Low-density polyethylene (PE, $\rho$ = 920 kg/m$^3$) was obtained from Quantam Chemicals, poly(hydroxy ester ether) (PHEE, $\rho$ = 1250 kg/m$^3$) was supplied by The Dow Chemical Company, and the granular starch filler ($\rho$ = 1500 kg/m$^3$) was obtained from Corn Products International. Before processing, the starch granules were dried to moisture content of <1%. No structural changes in starch were observed when starch/PHEE composites were extruded and injection molded at this low moisture content (14). Composites of starch/PE and starch/PE/PHEE were compounded on a Werner & Pfleiderer ZSK-30 twin-screw extruder. The temperature profile along the extruder barrel was typically 50, 130, 150, 155, 140, 130, 95°C and the screw speed was 200 rpm (17). However, the temperature profile was varied as needed in order to process composite materials with different filler contents. Starch and premixed blends of PE and PHEE pellets were separately metered gravimetrically into the extruder. The starch content in both the PE and in the PE/PHEE blend ranged from 0 to 70 weight percent and in the blends the PHEE content was fixed at 10 wt% of the matrix. Therefore, the PHEE content decreases as the weigh fraction of starch increases, while the PE/PHEE ratio is constant. The PHEE levels are comparable in magnitude to the 5 wt% needed for property enhancement observed by Ramkumar *et al.* (22). Unfilled blends of PE and PHEE were also prepared using the same experimental procedure. In these samples, the volume fraction of the minor component, PHEE, was less than 0.25.

Following compounding, dogbone-shaped tensile bars were injection molded using a Cincinnati Milacron ACT75B-113 80-ton injection molder. The temperature profile along the barrel was typically 85, 132, 160, 160°C with a sprue temperature of 180°C and a mold temperature of 45°C. For composites with filler fractions equal to or greater than 60 wt%, the sprue temperature was increased to 200°C and the mold temperature to 52°C (17). Following injection molding, the tensile bars were stored in plastic bags at 0°C to minimize moisture uptake. The samples were placed in the testing laboratory 12 h before performing the tests to ensure that the temperature within the bars was constant and equal to the testing temperature. The samples had a gauge length of 50.8 mm, a width of 12 mm and a thickness of 3.15 mm. All the tension tests were performed on an Instron universal testing frame, model 4201. Tests to failure were performed at a crosshead speed of 50 mm/min or a strain rate, $\dot{\varepsilon}$ of $1.64 \times 10^{-2}$ ($s^{-1}$). To measure the tensile modulus, the samples were also tested to a maximum strain, $\varepsilon = 0.1$, at $\dot{\varepsilon} = 3.3 \times 10^{-4}$ ($s^{-1}$). An Instron clip-on extensometer (series 2630-100) with a gauge length of 50.8 mm and a maximum travel of 5.08 mm was attached to the gauge length to record displacement. All tests were performed under controlled atmosphere of 21°C and 50% relative humidity. A minimum of five samples of each material was tested.

The tensile strength ($\sigma_u$) and the strain at failure ($\varepsilon_f$) were measured using the instrument software, Instron Series IX. To determine the yield stress ($\sigma_y$) and the tensile modulus (E), the experimental data was imported into the plotting program Sigma Plot. For all samples, the yield stress was defined as the stress that corresponds to the strain where the slope of the stress-strain curve ($\sigma$-$\varepsilon$) was first zero. The modulus was determined by measuring the slope of the $\sigma$-$\varepsilon$ curve at small strains.

The fracture surfaces of broken tensile bars were sputter coated with gold-palladium and examined using a JEOL JSM-6400V scanning electron microscope. To reveal the location and extent of debonding, as evidenced by reduction of translucency, the samples were placed on a fluorescent light box and photographed with a Kodak DCS 460c digital camera.

## RESULTS AND DISCUSSION

Representative stress-strain curves for the PE matrix and for selected filled composites with a total filler content, $\phi_f < 0.25$ and $\phi_f > 0.25$ are shown in *Figs. 1a* and *b*, respectively. For the starch-filled PE:PHEE blend, $\phi_f$ includes the granular starch, $\phi_s$, and the PHEE, $\phi_{PH}$, since this latter material is either dispersed in the matrix or encapsulates the starch granules (17).

In terms of engineering stress $\sigma$, the low-density PE matrix does not strain soften after yielding as shown in *Fig. 1a*. Instead there is a gradual increase in stress until the sample necks at high strains, $\varepsilon \sim 1.2$. Once a neck forms, the stress drops because of the reduction in cross-sectional area. Failure occurs when a crack forms within the necked region. The PE matrix also does not strain harden appreciably and so the tensile strength is approximately equal to the yield stress, $\sigma_u^m/\sigma_y^m = 1.15$.

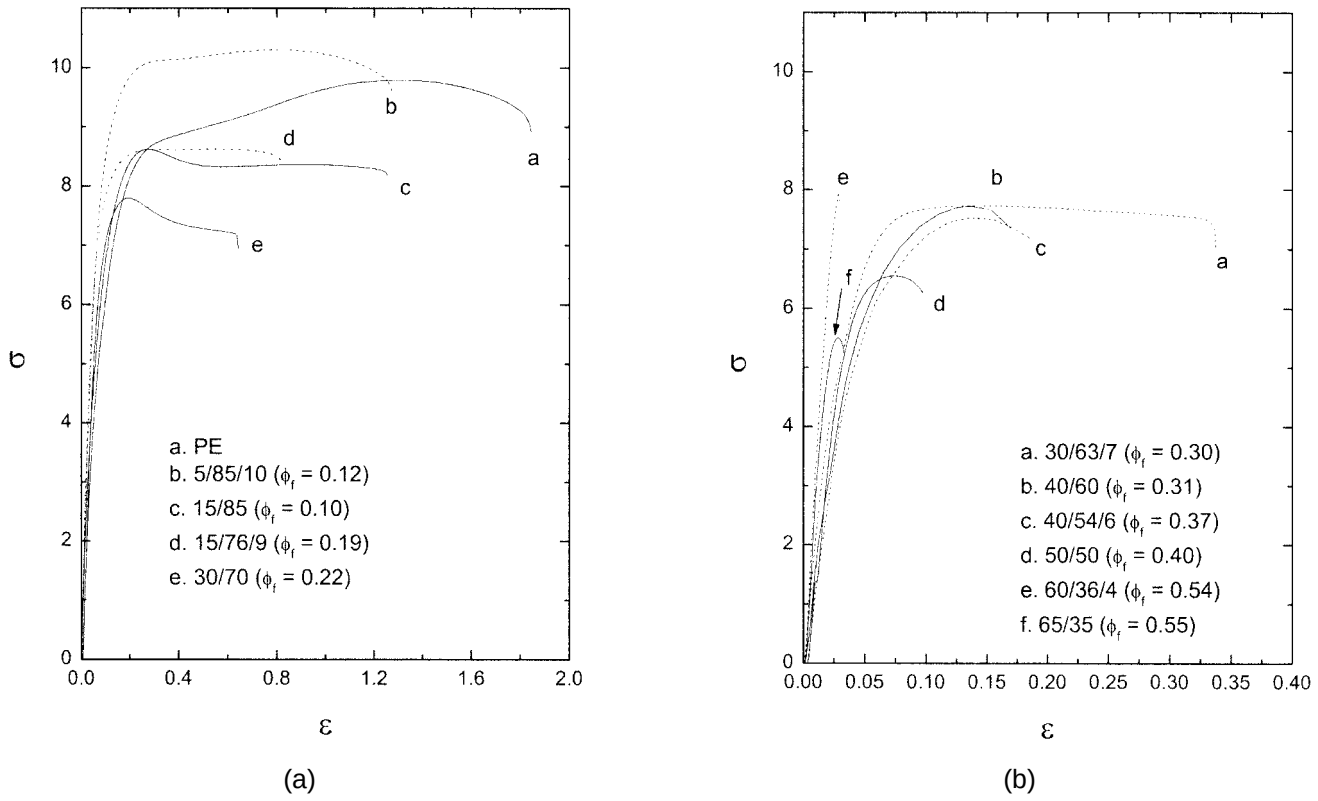


*Fig. 1. Stress (σ, MPa)-strain (ε) curves of selected starch-filled PE and starch-filled PE/PHEE blends with (a) $\phi_f < 0.25$ and (b) $\phi_f > 0.25$.*

The σ-ε curve for a starch filled PE:PHEE blend with $\phi_f < 0.15$ is very similar to the σ-ε curve for the PE matrix as shown in *Fig. 1a*. The absence of strain softening following yield point demonstrates that plastic deformation is not localized. Like the PE matrix, composites with small filler fractions do not neck at low strains. At filler contents above 0.15, the strain hardening evident in the unfilled matrix completely disappears. The samples deform at a constant stress and there is no local reduction in cross-sectional area. When $\phi_f > 0.35$, failure occurs at relatively low strains and the stress falls immediately following a maximum as shown in *Fig. 1b*. Once again, there is no evidence of necking, but all of the plastic deformation is restricted to the area immediately next to the fracture plane.

The addition of small amounts of starch filler to the PE matrix does not change the characteristics of the deformation process. The shape of the σ-ε curve for a sample with $\phi_f = 0.03$ is the same as the PE matrix shown in *Fig. 1a*. As the starch content increases, a broad but distinct maximum is evident at the yield stress. The strain softening that follows indicates that plastic deformation is localized. However, a distinct neck is not visible along the gauge length until high strains. When $\phi_f > 0.30$, the samples fracture before the stress drops to a constant value following yielding. This maximum is evident in all of the σ-ε curves until quasi-brittle failure occurs at $\phi_f = 0.55$.

The presence of a PHEE coating on the surface of the starch granules has a profound effect on the stress level at which nonlinear deformation begins. At low strains the tensile modulus of samples with similar $\phi_f$ are in agreement. This remains true at both high and low filler contents. However, at any strain beyond the initial linear portion of the σ-ε curve, the corresponding stress is lower in a starch/PE composite with the same filler content, as shown in *Fig. 1*. This decline in the secant modulus (instantaneous σ/ε) indicates that the starch/PE composites become permanently damaged at smaller strains. Similar changes in the σ-ε curves of other filled polymers have been observed when a coupling agent is added to improve interfacial adhesion (25). The influence of PHEE on the tensile properties is, therefore, analogous to the effect of a coupling agent.

In any filled polymer, debonding occurs over a specific stress interval that depends on the size of the filler particles, the interfacial strength and the filler volume fraction (26–29). In the starch-filled composites, the PHEE coating on the surface of the granules improves the interfacial strength and increases the debonding stress interval. This increase raises the composite yield stress, $\sigma_y^c$ as shown in *Fig. 2a*. At $\phi_f < 0.20$, $\sigma_y^c$ for the starch/PE/PHEE composites is greater than the yield stress of either a starch/PE composite or the unfilled PE matrix. Such an increase is possible only if the minimum de-bonding stress is greater than the yield

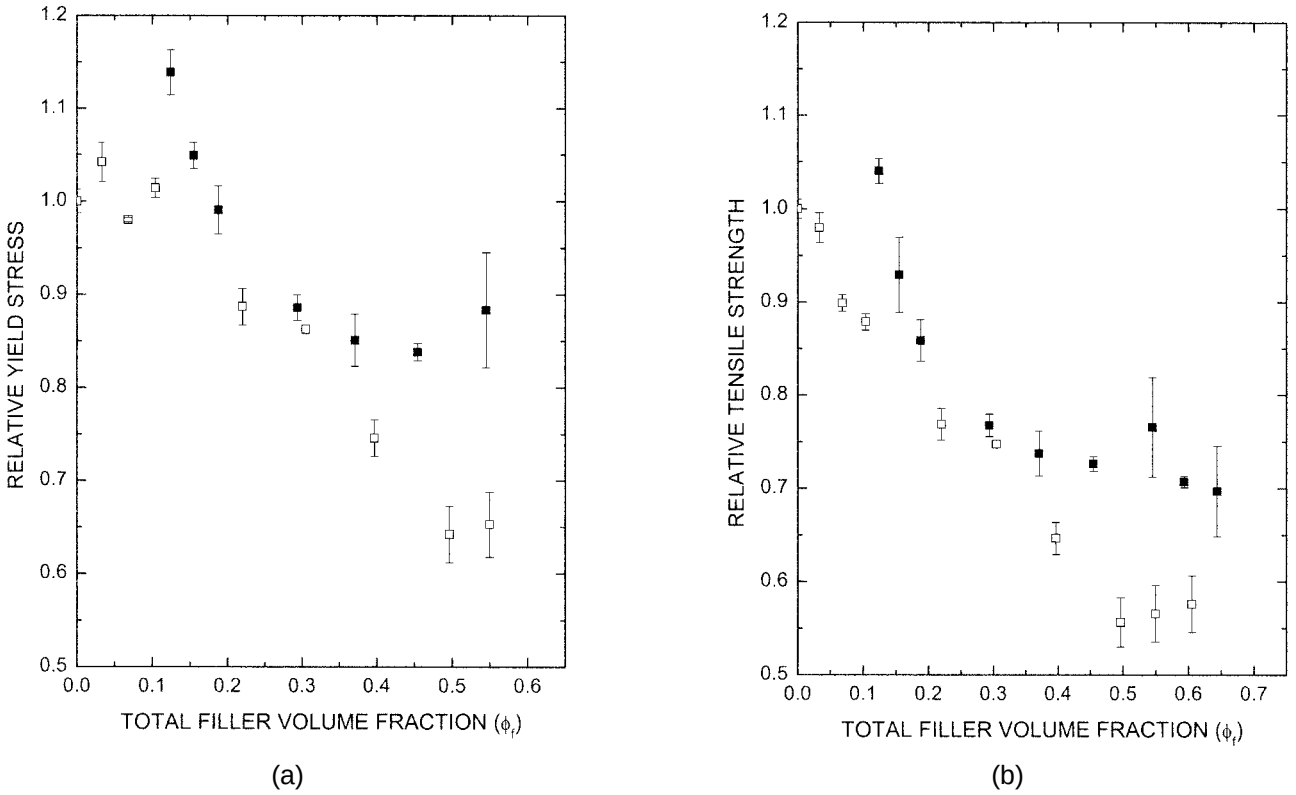


*Fig. 2. (a) Normalized composite yield stress, $\sigma_y^c$ vs. total filler content, $\phi_f$ and (b) normalized composite tensile strength, $\sigma_u^m$ vs. $\phi_f$ for starch-filled PE and for a starch-filled PE/PHEE blend. The yield stress and the tensile strength of the unfilled PE matrix are $\sigma_y^m = 8.6$ MPa and $\sigma_u^m = 9.9$ MPa.*

strength of the matrix, $\sigma_{dmin} > \sigma_y^m$ (27). For the starch/PE composites, the yield stress $\sigma_y^c$ remains approximately constant until $\phi_f > 0.10$, which indicates that at low filler contents, $\sigma_{dmin} \cong \sigma_y^m$. The presence of PHEE on the starch granules improves the interfacial adhesion or, more correctly, the interface between the PE and the PHEE is stronger than the interface between the PE and the starch granules.

In addition to the increase in yield stress, further evidence that matrix yielding precedes large scale debonding is provided from an examination of tensile bars tested to increasing initial strains $\varepsilon_i$. When $\varepsilon_i$ is less than the strain that corresponds to the yield stress, $\varepsilon_y \sim 0.25$, the entire gauge length has a uniform contrast following the removal of the applied stress, as shown in *Fig. 3*. In these starch-filled composites, stress whitening is the result of voiding around filler particles, which changes the transparency and alters the contrast when the samples are viewed using transmitted light. Uniform contrast indicates that there is no visible debonded region. When $\varepsilon_i > \varepsilon_y$, a stress-whitened region is apparent, which indicates that the samples are damaged. For example, debonding has occurred in the dark region in the upper half of the gauge length of a sample tested to $\varepsilon_i = 0.41$ as shown in *Fig. 3D*. As the initial strain increases, the size of the debonded region grows until it eventually encompasses the entire gauge length. Further extension then results in the formation of a neck and finally specimen failure. The general features of the deformation process are true for both materials with filler content less than ~0.30, except that the samples no longer neck before fracturing at high extensions when $\phi_f > 0.15$.

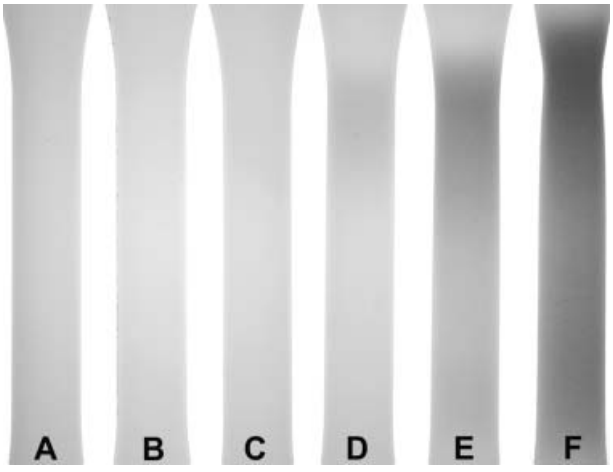


*Fig. 3. Optical photographs of a starch/PE/PHEE composite with $\phi_f = 0.12$ tested to increasing strains, $\varepsilon_i$. (A) $\varepsilon_i = 0$, (B) $\varepsilon_i = 0.20$, (C) $\varepsilon_i = 0.25$, (D) $\varepsilon_i = 0.41$, (E) $\varepsilon_i = 0.80$, and (F) $\varepsilon_i = 1.20$.*

If the matrix yields before the onset of debonding, this would occur close to the poles of a filler particle where the stress concentration factor is largest, $k \sim 2$ (30, 31). With increasing $\varepsilon$, the stress within this locally yielded material increases because it strain-hardens. This process of local yielding followed by strain-hardening continues until the local stresses are greater than the strength of the polymer/filler interface. At this point, the starch granules debond from the matrix. Further extension results in the growth of this porous zone provided that neighboring granules can be detached from the matrix. Debonding will also occur away from the initially damaged region as the stress increases. Following the formation of a debonded region, subsequent deformation involves a secondary debonding process occurring at the interface between the damaged and undamaged zones. The growth of the damaged zone will depend on a competition between the debonding stress, $\sigma_d$, and the stress within the damaged porous zone, $\sigma_{dz}$. If $\sigma_{dz} > \sigma_d$, then the porous zone grows, but if $\sigma_{dz} < \sigma_d$, then further extension will be confined to the already damaged material. In this case the polymer ligaments within the porous zone are extended as the strain increases. Eventually, when the strain within these ligaments equals the strain at failure of the unfilled matrix, they fracture. A crack is formed by the coalescence of extended pores created by the fracture of drawn polymer ligaments. Extension of the polymer ligaments within the porous region results in the formation of a neck at high strains as shown in *Fig 3F*.

The stress within the damaged zones depends on the volume fraction of pores and on the strength of the polymer ligaments. Since these zones extend across the entire cross section of the sample, the Nicolais-Narkis model can be used to describe the stress $\sigma_{dz}$ within them (32):

$$\sigma_{dz} = \sigma_s(1 - \alpha\phi_p^{2/3}) \quad (1)$$

where $\sigma_s$ is the stress in the polymer ligaments, $\alpha$ is a constant that accounts for partial transmission of the load to the filler particles and $\phi_p$ is the pore concentration. *Equation 1* was used by Dubnikova *et al.* (27) to describe the decrease in composite tensile strength of filled polymer composites. The original model of Nicolais and Narkis assumes no stress transfer to the filler particles, and $\alpha$ is simply related to the maximum packing fraction of the filler. According to the model, the tensile strength decreases because of a reduction in the effective cross-sectional area after the filler particles debond. The decline in both $\sigma_y^c$ and $\sigma_u^c$, shown in *Fig. 2*, demonstrates that *Eq 1* is applicable over a range of $\phi_f$ for both starch-filled composites. For both there is an increase in the pore concentration with increasing filler content and a corresponding decline in the tensile strength.

Changes in the composite tensile strength, $\sigma_{u,}^c$ with filler content mimic the changes in the yield strength as shown in *Fig. 2b*. For the starch-filled blend there is an increase in $\sigma_u^c$ at small $\phi_f$. However, once the filler content exceeds ~0.10, the tensile strength decreases until $\phi_f > 0.30$. At higher filler contents, $\sigma_u^c$ remains constant and is equal to ~0.75 $\sigma_u^m$ or 0.85 $\sigma_y^m$. For the starch/PE composites $\sigma_u^c$, unlike $\sigma_y^c$, falls continually until $\phi_f = 0.50$. Above this value the tensile strength remains constant and is equal to approximately 0.6 $\sigma_u^m$ or 0.65 $\sigma_y^m$.

The higher tensile strength of the starch-filled PE: PHEE blend, at large $\phi_f$, is further indication of an increase in interfacial adhesion. This increase can be illustrated by examining the fracture process at high filler contents, $\phi_f > 0.40$. In both materials, failure occurs immediately following the onset of debonding, i.e. all of the deformation occurs within a narrow damaged zone as shown in *Figs. 4* and *5*. When the samples fail in this manner, their tensile strength equals the minimum debonding stress, $\sigma_{dmin}$ (27). The higher $\sigma_u^c$ of the filled blend indicates that the debonding stress is higher for this material. For both composite materials $\sigma_{dmin} < \sigma_y^m$ at high $\phi_f$, which contradicts the observation that at low filler contents $\sigma_{dmin} > \sigma_y^m$. The minimum debonding stress appears to decrease at high filler fractions, which may be the result of particle agglomeration. Larger filler particles have been shown to have a smaller minimum debonding stress (27). Particle clusters can be found on the fracture surface of starch/PE/PHEE composites with a filler content above 0.20 (17).

For the starch/PE/PHEE composites, the deformation process changes at a filler content of 0.37. When $\phi_f$ is less than this critical filler value $\phi_{cr}$, deformation involves secondary debonding and the subsequent growth of the damaged zone(s). Above $\phi_{cr}$, deformation is concentrated within narrow damaged zones that lie perpendicular to the direction of applied stress as shown in *Fig. 4*. These damaged zones are highly compliant


*Fig. 4. Optical photographs of fractured tensile bars of starch/PE/PHEE composites with (A) $\phi_f = 0.30$, (B) $\phi_f = 0.37$ and (C) $\phi_f = 0.45$.*


*Fig. 5. Optical photographs of fractured tensile bars of starch/PE composites with (A) $\phi_f = 0.22$, (B) $\phi_f = 0.31$, (C) $\phi_f = 0.40$, and (D) $\phi_f = 0.50$.*

because of the large pore concentration. Outside of the damaged zones, the filler particles remain firmly bonded and the matrix experiences only minimal extension. For the starch-filled PE/PHEE blend, $\phi_{cr}$ also corresponds to the filler content above which the tensile strength remains constant. There is also a change in the deformation process in the starch filled PE composites; however, it occurs at a lower filler content, $\phi_{cr} = 0.31$ as shown in *Fig. 5*. In contrast to the behavior of the filled blend, the tensile strength continues to decrease after the deformation process becomes confined to narrow damaged zones. The decline in $\sigma_u^c$ and the shift in $\phi_{cr}$ towards lower filler contents are both due to the weaker interface between the filler and the matrix in the binary composite.

In these starch-filled composites, the effect of interfacial strength on the debonding process can be understood using *Eq 1*. At $\phi_f = 0.30$, deformation in the starch-filled PE/PHEE blend involves secondary debonding so $\sigma_{dz} > \sigma_d$. But at the same $\phi_f$, the deformation in a starch/PE composite is confined to the initial debonded zone so $\sigma_{dz} < \sigma_d$. Since these materials have the same $\phi_f$ and the same PE matrix, $\phi_p$ and $\sigma_s$ should be equivalent. Then, according to *Eq 1*, the difference in their respective $\sigma_{dz}$ is due to a difference in the value of $\alpha$, which depends on how efficiently the stress is transferred to the filler particles. In order for $\sigma_{dz}$ for the starch/PE/PHEE composites to be larger than $\sigma_{dz}$ for the starch/PE composites, its corresponding $\alpha$ must be smaller. A smaller $\alpha$ is an indication of improved adhesion since this parameter approaches zero in the case of perfect adhesion (33). Estimates of $\alpha$ for the starch-filled PE are 0.60 ($\sigma_u$) and 0.36 ($\sigma_y$), and 0.45 ($\sigma_u$) and 0.30 ($\sigma_y$) for the starch/PE/PHEE composites. The value of $\alpha$ for $\sigma_u$ of the starch/PE materials is similar to the value estimated from the data of Willett (21). The increase in interfacial strength is even more significant considering the higher debonding stress in the starch-filled PE/PHEE blend.

For both composite materials, once debonding becomes confined to narrow deformation zones there is a large decrease in the strain at failure, $\varepsilon_f$. For the starch-filled PE, $\varepsilon_f$ decreases by approximately a factor of four at $\phi_{cr}$ as shown in *Fig. 6*. In the case of the starch-filled blend, the decline in $\varepsilon_f$ is more gradual since it occurs at higher $\phi_f$. For both materials, once debonding becomes confined, $\varepsilon_f$ continues to drop, owing to the reduction in the number of damaged zones as shown in *Fig. 4* and *Fig. 5*. Similar changes in the debonding process have been found in other filled polymers (26–28).

Despite the changes in the deformation process, fracture involves debonding of the starch granules and extension of the surrounding polymer ligaments for both composite materials at all filler contents. At low $\phi_f$, the fracture surface is characterized by extended polymer ligaments and elongated voids as shown in *Fig. 7A* for a starch-filled blend with a filler content of 0.12. The matrix strands are highly drawn. As the filler content increases, the fracture surface becomes smoother, reflecting the decline in ductility, as shown in *Fig. 7B* for the starch-filled blend with $\phi_f = 0.45$. Even at this large

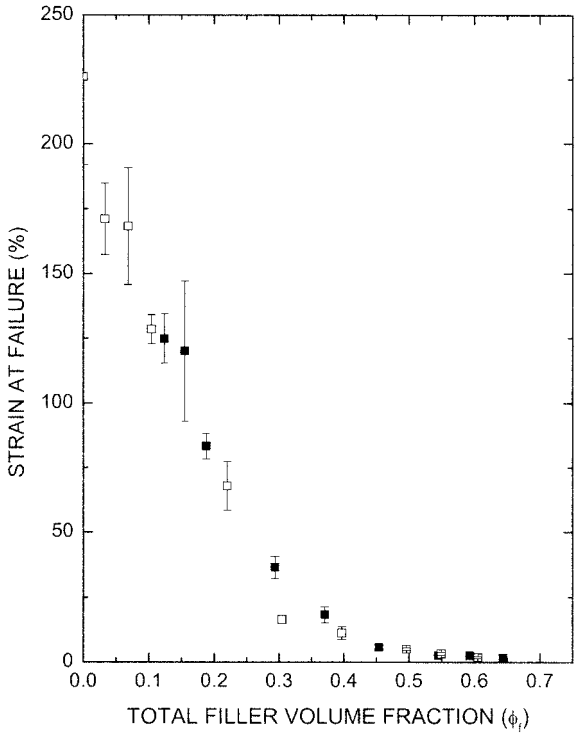


*Fig. 6. Strain at failure, $\varepsilon_f$ versus total filler content, $\phi_f$ for starch-filled PE and for a starch-filled PE/PHEE blend. Open symbols are starch/PE; filled symbols are starch/PE/PHEE.*

$\phi_f$, highly drawn polymer ligaments are still found between debonded starch granules. Relatively short but drawn polymer ligaments can be seen on the fracture surface at the highest $\phi_f$ as shown in *Fig. 7C*. At all filler contents, fracture occurs within a zone of damaged material consisting of debonded starch granules and drawn polymer ligaments. For the starch-filled blend, the coating on the surface of the granules indicates that the interface between starch and PHEE is stronger than the interface between PE and PHEE. In this material, debonding involves separation of the matrix from the PHEE interlayer.

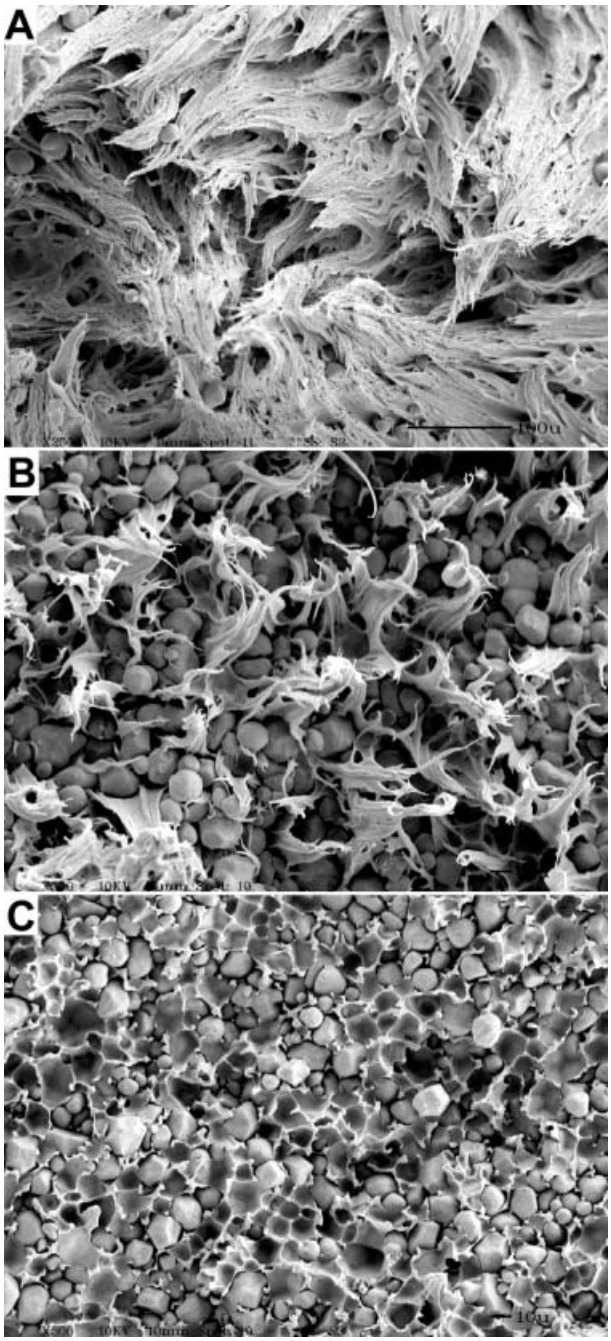


*Fig. 7. SEM micrographs of fracture surfaces of starch-filled PE/PHEE blend with (A) $\phi_f = 0.12$; (B) $\phi_f = 0.45$; and (C) $\phi_f = 0.63$. Magnifications are 250× in (A) and 500× in (B) and (C).*

In addition to affecting the ultimate properties, a surface coating on the filler particles may also change the composite modulus (3, 34). For both binary and ternary composites, the increase in the tensile modulus $E_c$ with $\phi_f$ can be described using a variety of different models including the Kerner equation (1). If the filler particles are spherical, then this equation has the form:

$$E_c = E_m\left(\frac{1 + AB\phi_f}{1 - B\varphi\phi_f}\right) \tag{2}$$

where $E_m$ is the Young's modulus of the matrix and the constants $\varphi$, A and B are defined as follows:

$$\varphi = 1 + \frac{1 - \phi_{max}}{\phi_{max}^2}\phi_2 \tag{3}$$

$$A = \frac{7 - 5\nu_m}{8 - 10\nu_m} \tag{4}$$

$$B = \frac{E_f/E_m - 1}{E_f/E_m + A} \tag{5}$$

where $\phi_{max}$ is the maximum packing fraction of filler, $E_f$ is the Young's modulus of the filler and $\nu_m$ is the matrix Poisson's ratio (0.43). For granular starch $\phi_{max} = 0.65$ (35) and $E_s = 15$ GPa (21). An upper and lower limit for the tensile modulus of the PHEE-coated starch granules can be estimated using the following equations:

$$E_{fp} = \phi_o E_{PH} + (1 - \phi_o)E_s \tag{6a}$$

$$\frac{1}{E_{fs}} = \frac{\phi_o}{E_{PH}} + \frac{(1 - \phi_o)}{E_s} \tag{6b}$$

where $E_f$ is the modulus of the composite filler determined by the parallel (p) or series (s) models, $E_{PH}$ is the modulus of PHEE (2200 MPa), and $E_S$ is the starch modulus. For these core-shell filler particles, the volume fraction of the outer PHEE layer, $\phi_o$, can be estimated from the known volume fractions of PHEE and starch, $\phi_o = \phi_{ph}/(\phi_{ph} + \phi_s)$ if it is assumed that all of the PHEE encapsulates the starch granules (17). If a portion is dispersed in the matrix, then this relationship will overestimate the volume fraction of the outer shell, and the actual filler modulus will be larger than the estimate since $E_{PH} < E_s$.

Modulus data for both composite materials are shown in *Fig. 8*. Also shown are the predictions of *Eq 2* as well as the Kerner equation approximation for materials with $E_f \gg E_m$ (1). In this case *Eq 2* reduces to:

$$\frac{E_c}{E_m} = 1 + \frac{15(1 - \nu_m)}{8 - 10\nu_m}\frac{\phi_f}{(1 - \phi_f)} \tag{7}$$

For the starch-filled blend, the filler modulus was estimated using both forms of *Eq 6*. *Equation 2* fits the experimental data well up to $\phi_f \approx 0.45$ for the three values of $E_f$, while at higher filler fractions, it exceeds the

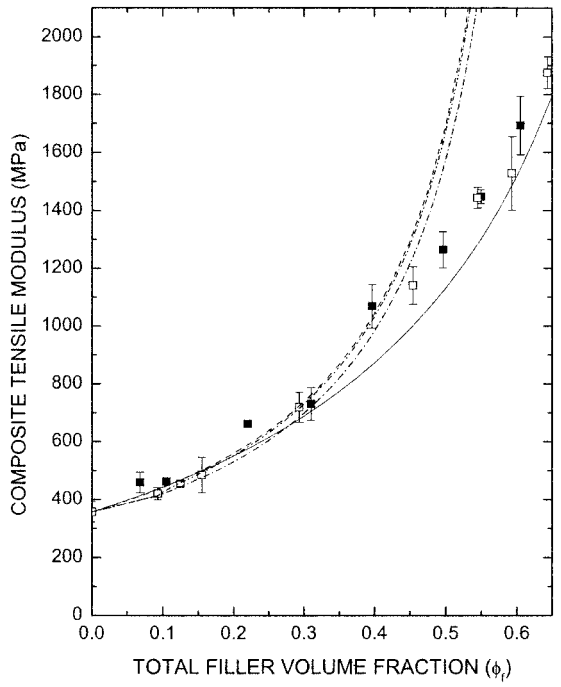


*Fig. 8. Composite tensile modulus $E_c$ versus total filler content $\phi_f$ for starch-filled PE and starch-filled PE/PHEE blends. Open symbols are starch/PE; filled symbols are starch/PE/PHEE. Predicted modulus using Eq 2 with $E_f = E_s$ (— —); $E_f$ calculated using Eq 6a (— · ·); $E_f$ calculated using Eq 6b (— ·). The solid line is Eq 7.*

experimental data. However, at all $\phi_f$, the simplified form of the Kerner equation adequately describes the experimental data for both composite materials. The lack of fit between *Eq 2* above $\phi_f \approx 0.45$ and the data may reflect the presence of agglomerated starch granules at higher starch contents (17). The presence of a PHEE coating on the surface of the starch granules does not significantly change the room temperature composite modulus. This result is not unexpected given the small volume fraction of PHEE, particularly at high starch contents, and given that the PHEE is more rigid than the PE matrix.

## CONCLUSIONS

A PHEE coating on the surface of starch granules increases the tensile strength and the yield strength at both high and low filler contents. At low filler contents, the yield stress of a starch/PE/PHEE composite is greater than the yield stress of the unfilled PE matrix, which indicates that the matrix yields before the starch granules debond. In the starch/PE composites, the yield stress remains constant at low $\phi_f$, which again suggests that debonding begins after the matrix yields. As the filler content increases, the tensile strength of both materials decreases until it becomes constant at large $\phi_f$. For the starch-filled blend this occurs at $\phi_f$ = 0.31, but for the starch/PE composites this is not the case until $\phi_f$ = 0.50. The constant tensile strength at large $\phi_f$ can be used as an estimate of the minimum debonding stress since failure occurs immediately following the onset of debonding. The minimum debonding stress is larger for the starch-filled PE/PHEE blend, which again indicates that the filler/matrix interface is stronger. In both composite materials there is a transition in the debonding process at a critical filler content, $\phi_{cr}$. Below $\phi_{cr}$, deformation involves the growth of damaged region by secondary debonding. Above this critical filler content, deformation is restricted to narrow damaged zones. Once this transition in the deformation process occurs, there is a large decrease in the strain at failure of both composites. Although a PHEE coating affects the tensile strength, it does not significantly change the room temperature tensile modulus. Therefore, in these filled composites, a PHEE coating on the surface of the starch granules acts as a compatibilizer, which increases the tensile strength, but does not lower the strain at failure or the tensile modulus.

## ACKNOWLEDGMENTS

The authors thank S. Myers and M. Mitchell for their assistance with the compounding and injection molding and Dr. A. Thompson for scanning electron microscopy. This research was conducted under Cooperative Research and Development Agreement 58-3K95-8-633 between ARS and Biotechnology Research Development Corporation.

## REFERENCES

1. L. E. Nielsen and R. F. Landel, *Mechanical Properties of Polymers and Composites—2nd Ed.*, Marcel Dekker, Inc. (1994).
2. J. Kolarik and J. Jancar, *Polymer*, **33**, 4961 (1992).
3. D. Benderly, A. Siegmann, and M. Narkis, *J. Mater. Sci. Let.*, **14**, 132 (1995).
4. J. Wang, J. F. Tung, M. Y. Ahmad Fuad, and P. R. Hornsby, *J. Appl. Polym. Sci.*, **60**, 1425 (1996).
5. S. Y. Hobbs, M. E. J. Dekkers, and V. H. Watkins, *Polymer*, **29**, 1598 (1988).
6. G. Marosi, G. Bertalan, P. Anna, and I. Rusznak, *J. Polym. Eng.*, **12**, 33 (1993).
7. D. Benderly and A. Siegmann, *Polym. Compos.*, **17**, 86 (1996).
8. N. D. Alberola, Y. Germain, and P. Mele, *J. Appl. Polym. Sci.*, **63**, 1041 (1997).
9. P. S. Walia, J. W. Lawton, R. L. Shogren, and F. C. Felker, *Polymer*, **41**, 8083 (2000).
10. G. Zhou, J. L. Willett, and C. J. Carriere, *Polym. Eng. Sci.*, **41**, 1365 (2001).
11. G. Biresaw and C. J. Carriere, *J. Polym. Sci. Part B*, **39**, 920 (2001).
12. C. Wang, C. J. Carriere, and J. L. Willett, *J. Polym. Sci. Part B*, **40**, 2324 (2002).
13. P. S. Walia, J. W. Lawton, and R. L. Shogren, *J. Appl. Polym. Sci.*, **84**, 121 (2002).
14. J. L. Willett and W. M. Doane, *Polymer*, **43**, 4413 (2002).
15. R. L. Shogren, W. M. Doane, D. Garlotta, J. W. Lawton, and J. L. Willett, *Polym. Deg. Stab.*, **79**, 405 (2003).
16. D. Garlotta, W. M. Doane, R. L. Shogren, J. W. Lawton, and J. L. Willett, *J. Appl. Polym. Sci.*, **88**, 1775 (2003).
17. S. St. Lawrence, P. S. Walia, and J. L.Willett, *Polym. Eng. Sci.*, **43**, 1250 (2003).

18. R. L. Evangelista, Z. L. Nikolov, W. Sung, J.-L. Jane, and R. J. Gelina, *Ind. Eng. Chem.*, **30**, 1841 (1991).
19. J.-L. Jane, A. W. Schwabacher, S. N. Ramrattan, and J. A. Moore, U.S. Patent 5,115,000 (1992).
20. J. L. Willett, U.S. Patent 5,087,650 (1992).
21. J. L. Willett, *J. Appl. Polym. Sci.*, **54**, 1685 (1994).
22. D. H. S. Ramkumar, M. Bhattacharya, and U. R. Vaidya, *Eur. Polym. J.*, **33**, 729 (1997).
23. R. R. N. Sailaja and M. Chanda, *J. Appl. Polym. Sci.*, **80**, 863 (2001).
24. H.-M. Park, S.-R. Lee, S. R. Chowdhury, T.-K. Kang, H.-K. Kim, S.-H. Park, and C.-S. Ha, *J. Appl. Polym. Sci.*, **86**, 2907 (2002).
25. E. A. A. van Hartingsveldt and J. J. van Aartsen, *Polymer*, **30**, 1984 (1989).
26. I. L. Dubnikova, V. G. Oshmyan, and A. Y. Gorenberg, *J. Mater. Sci.*, **32**, 1613 (1997).
27. I. L. Dubnikova and V. G. Oshmyan, *Polym. Sci., Ser. A*, **40**, 925 (1998).
28. I. L. Dubnikova, D. K. Muravin, and V. G. Oshmyan, *Polym. Eng. Sci.*, **37**, 1301 (1997).
29. A. V. Zhuk, N. N. Knunyants, V. G. Oshmyan, Y. A. Topolkaraew, and A. A. Berlin, *J. Mater. Sci.*, **28**, 4595 (1993).
30. J. N. Goodier, *Trans. ASTM*, **55**, 7 (1933).
31. L. Sinien, Y. Lin, Z. Xiaoguang, and Q. Zongneng, *J. Mater. Sci.*, **27**, 4633 (1992).
32. L. Nicolais and M. Narkis, *Polym. Eng. Sci.*, **11**, 194 (1971).
33. P. Godard, Y. Bomal, and J. J. Biebuyck, *J. Mater. Sci.*, **28**, 6605 (1993).
34. V. A. Matonis, *Polym. Eng. Sci.*, **9**, 90 (1969).
35. J. L. Willett, *Cereal Chem.*, **78**, 64 (2001).